A comparison of synchrotron X-ray phase contrast tomography and holotomography for non-invasive investigations of the internal anatomy of mites

Michael Heethoff[1]*& Peter Cloetens[2]

[1]*Universität Tübingen, Abteilung für Evolutionsbiologie der Invertebraten, Auf der Morgenstelle 28E, 72076 Tübingen, Germany; e-mail: Heethoff@gmx.de*

[2]*European Synchrotron Radiation Facility, B.P. 220, 38043 Grenoble, France*

* *Corresponding author*

Abstract

Synchrotron X-ray tomography is a powerful tool for non-invasive studies of the internal anatomy of microarthropods. The invention of phase contrast imaging (PCT) enables the visualisation of biological tissues with a small range of attenuation coefficients. Quantitative phase tomography (holotomography; HT) is an advancement of PCT and improves the imaging quality of materials with even smaller differences in attenuation coefficients. In this study, HT was used for the first time to investigate the internal anatomy of microarthropods. Both techniques, HT and PCT, are compared with respect to their ability to differentiate between soft tissues with low attenuation coefficients of the oribatid mite *Archegozetes longisetosus* (Acari, Oribatida). HT has a higher signal-to-noise ratio and a broader grey value distribution and resolves slight variations in soft tissues much better than PCT.

Keywords: Acari, Oribatida, µCT, X-ray imaging

Zusammenfassung

Synchrotron-Röntgentomographie ist eine wichtige neue Methode für nicht-invasive Untersuchungen der inneren Anatomie von Mikroarthropoden. Durch die Verwendung von Phasenkontrast (PCT) können auch biologische Gewebe mit sehr niedriger Röntgendichte sichtbar gemacht werden. Holotomographie (HT) ist eine methodische Weiterentwicklung der Phasenkontrasttomographie zur Verbesserung der differenziellen Darstellungsqualität verschiedener Gewebetypen. Dies ist die erste Studie, in welcher HT zur Untersuchung der inneren Anatomie von Microarthropoden verwendet wurde. Die Darstellungsqualität beider Methoden (PCT und HT) anhand verschiedener Gewebetypen bei der Hornmilbe *Archegozetes longisetosus* (Acari, Oribatida) wird verglichen. HT hat ein besseres Signal/Rausch-Verhältnis als PCT und eine breitere Grauwertverteilung; daher werden verschiedene Gewebetypen deutlich besser aufgelöst als bei PCT.

1. Introduction

Knowledge of the internal anatomy of organisms is fundamental for understanding their functional biology and evolution. Information on the internal organisation is traditionally obtained by dissecting or histological serial sectioning, both of which are destructive for the sample to be analysed (Betz et al. 2007). Histological sections can be stained with different techniques and then viewed by light or transmission electron microscopy. The spatial resolution of a light microscope is 300 nm, that of a transmission electron microscope is 1 nm. While these microscopical techniques are suitable for planar 2-D-objects, scanning electron microscopes (SEM) can be used to image the surfaces of 3-D-objects with a high focal depth and a spatial resolution of about 5 nm. However, SEM is only suitable for surfaces and does not provide information about the internal organisation of the samples.

An imaging technique which provides information on the internal and external organisation of a sample without the need of dissection or serial sectioning is X-ray computer tomography, developed by Allen M. Cormack and Godfrey Hounsfield in the 1960s. Both were awarded with the Nobel Prize in Medicine in 1979. Since then, computer tomography became one of the most important imaging techniques in medical applications, and modern devices are suitable for resolutions of ~ 0.3 mm. While this resolution is sufficient for imaging of large samples, it is by far too low for investigations on microarthropods, with a body size even below the resolution of these devices (the whole sample would fit in less then ten pixel).

Medical devices generate X-rays with an X-ray tube by accelerating electrons from a cathode in a strong electric field onto a metallic anode where electrons from the inner shells of the anodic atoms are knocked out and the vacancies are filled up with electrons from higher energy levels. Hereby, they cause the characteristic X-rays with a typical wavelength for any anodic material. Another type of X-rays is produced by those electrons which do not hit other electrons of the anode but are instead scattered by the electric field of the nuclei of the anodic atoms. In contrast to the characteristic X-rays, this so-called bremsstrahlung has a wide spectrum of electromagnetic radiation.

Besides in X-ray tubes, the equivalent of bremsstrahlung can also be produced in a synchrotron. Here, electrons are produced by an electron gun and accelerated in a circular booster ring until they reach an energy level of up to 6 GeV (at the European Synchrotron radiation facility, ESRF, Grenoble, France). From here they are transferred to a storage ring where they circulate with a velocity close to that of the speed of light. The storage ring is build up by linear and curved parts. Electrons are bent by dipole magnets whenever a linear part meets a curved part of the ring. This bending results in a deceleration of the electrons and thereby in the generation of synchrotron radiation, consisting of a wide spectrum from microwaves to hard X-rays. In modern, third generation synchrotron facilities, there are in addition insertion devices in the linear parts of the ring. These are periodic arrays of alternating dipole magnets (undulators) and produce sharp energy levels (Betz et al. 2007). By using synchrotron radiation, tomographic imaging becomes possible with a pixel-resolution of down to 270 nm, thus comparable to a light microscope. The resolution depends on the sample size and is well suitable for the analyses of microarthropods and other micro-scaled materials (Weide & Betz 2007).

A severe problem for imaging biological materials with X-rays is the contrast mechanism.Traditionally in medical applications, absorption is used with almost no distance between sample and detector. The intensity of the beam decreases exponentially with

increasing propagation distance, depending on the X-ray attenuation coefficient of the material. The attenuation coefficient is a function of the electron density of the material and the atomic number of its chemical elements. Hence, homogeneous materials with a low attenuation coefficient or heterogeneous materials with a small range of attenuation coefficients will produce insufficient contrast for absorption imaging.

For such materials, phase contrast tomography (PCT) enhances the imaging quality by using a certain distance between the sample and the detector (Cloetens et al. 1996). Phase contrast imaging, however, requires a homogeneous and spatially coherent beam which is generated with high quality by insertion devices of third generation synchrotrons. Phase contrast is possible due to the fact that the beam is not only absorbed by the material but that the phase of the wave is also affected, depending on the materials refractive index. A certain distance is needed between sample and detector for phase contrast because the phase shift does not influence the amplitude of the wave and is thus not detectable in the absorption region (Betz et al. 2007).

While PCT is based on a single distance between the detector and the sample, holotomography (HT) uses a combination of several distances and combines the phase shift information to produce phase maps which are subsequently used for the tomographic reconstruction (Cloetens et al. 2007). This technique is helpful when the materials of interest have very small variations in attenuation coefficients which lead to insufficient imaging results even with phase contrast techniques.

It is important to note that X-ray imaging does not produce 3-D images directly. Instead, a series of 2-D-images (radiographs) is produced which is then used to calculate 3-D volume data. The radiographs contain no depth information and are an integration of the linear attenuation coefficient along the propagation path of the beam. To obtain 3-D-information, radiographs from a number of different angles (0° – 180°) have to be obtained from the sample, concatenated into sinograms for each line of the detector and finally reconstructed with a filtered back projection algorithm which is based on Radon's theorem (Radon 1917). The resulting voxel-dataset (3-D-pixel) can be analysed using volume graphics software.

Here, PCT and HT are compared for their use to differentiate between different soft tissues with a low range in X-ray attenuation coefficients in a microarthropod with less than 1 mm body size (*Archegozetes longisetosus* Aoki, Acari, Oribatida).

2. Materials and methods

2.1. Animals used in this study

Specimens of the parthenogenetic oribatid mite *Archegozetes longisetosus* were taken from our laboratory culture. This genetic strain was established by Roy A. Norton in 1993 from a single gravid female collected from decomposing coconut debris at Lucillo (Puerto Rico), and was denoted *A. longisetosus* ran (Heethoff et al. 2007). The culture grows on a plaster of Paris/charcoal mix (9:1) in plastic jars, in constant dark at 23 °C with approximately 90 % of air humidity. Bark from different trees with unicellular algae (mainly *Protococcus*) growing on them is provided as food and replaced twice a week.

2.2. Synchrotron X-ray tomography and holotomography

Fresh specimens were taken from the culture, cleaned with a fine brush and placed in a 6:3:1 mixture of 80 % ethanol, 35 % formaldehyde and 100 % acetic acid for 24 hours. Specimens were then dehydrated in a graded ethanol series of 70 %, 75 %, 80 %, 85 %, 90 %, 95 %, and 100 % with 3 changes at each concentration, and 10 min between the steps. Finally, samples were placed in fresh 100 % ethanol overnight and critical point dried in CO_2 (CPD 020, Balzers). Dried specimens were attached to the tip of a plastic pin (1.2 cm long; 3.0 mm in diameter). X-ray tomography was performed at beamline ID19 (ESRF, Grenoble, France, experiment SC-2127) with an energy of 20.5 keV. The radiographs were recorded with a cooled CCD (ESRF FReLoN camera) with a 14-bit dynamic range, 2048 × 2048 pixels and an effective pixel size of 0.7 μm. 1500 projections were recorded over the 180° sample rotation with an exposure time of 0.35 s for each projection. The detector-to-sample distance was 20 mm for phase contrast imaging and 10 mm, 20 mm and 45 mm for holotomography. Data were converted to 8-bit grey values and the distribution of grey values was analysed with ImageJ 1.38X (http://rsb.info.nih.gov/ij/). The comparison of PCT and HT was mainly based on the distribution and the range of grey values in the virtual slices. Two criteria were used to quantify the quality of images: i) range of grey values within the tissue, ii) distance between mean grey values of the sample and the background. The higher the range of grey values was within a specific tissue, the better was the differentiation among parts of the tissue. The higher the distance was between grey values of the background and the sample, the better was the overall-information of the image (higher signal-to-noise-ratio).

3. Results

3.1. General comparison of phase contrast tomography (PCT) and holotomography (HT)

The reconstructed virtual slices consisted of grey values with an 8-bit range (256 values), where the grey value '0' was black and '255' white. The background of PCT images ranged from 90 to 115 (max.: 102, mean: 101, SD: 1.8; Fig. 1A). The background of HT images ranged from 193-230 (max.: 221, mean: 215.4, SD: 7.1; Fig. 1C). A cross-sectional virtual slice in the region of the ovary and posterior part of the ventriculus was used to compare the general distribution of grey values within the sample and the surrounding background (Figs 1B, D). In the PCT slice, all grey values (0 – 255) were present to some extent (max.: 102, mean: 101.8, SD: 11.4) while the HT slice consisted only of grey values ranging from 0 to 244 (max.: 221, mean: 201.6, SD: 40.5). The histograms had a peak-like shape for PCT but were more complexly distributed for HT.

The grey value distribution was also compared along a path crossing a part of the cuticle of the exoskeleton (Fig. 2). PCT produced edge enhancement at the borders of materials with different attenuation coefficients. This led to an artificial darker 'layer' on both sides of the material. This edge enhancement was not observable in HT images (Fig. 2).
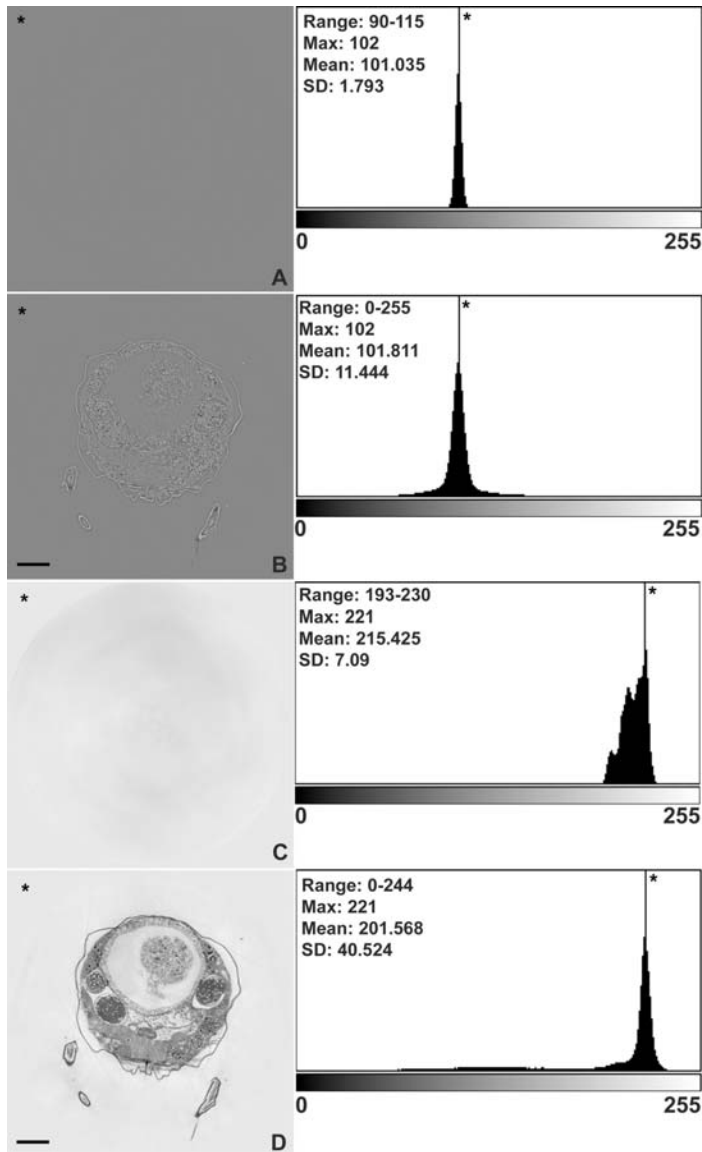
Fig. 1   Comparison of grey value distribution in virtual slices of PCT and HT of the background and the sample. Left row (A – D) shows the reconstructed slices, right row shows the corresponding histograms. A: PCT background; B: PCT sample; C: HT background; D: HT sample. Asterisk: Artificial corners in the reconstructed slices and corresponding grey values. Bar: 100 µm.
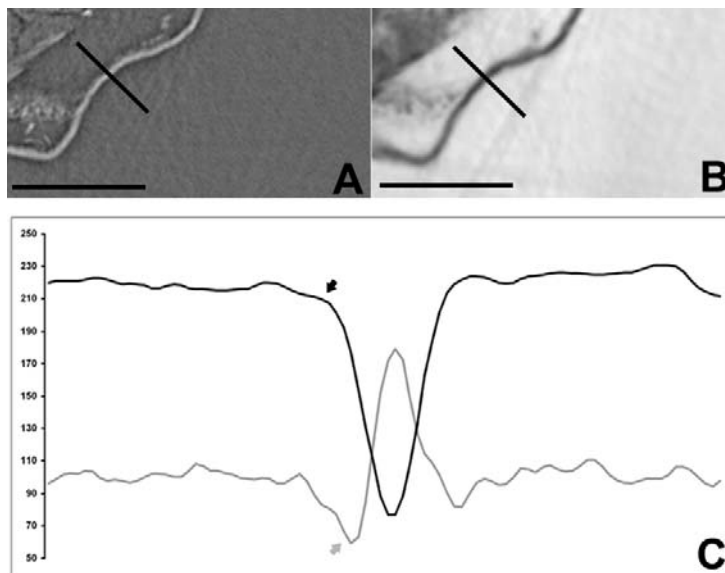
Fig. 2   Comparison of grey value distribution along a path crossing the cuticle (black line). A: PCT;
              B: HT; C: distribution of grey values along the path, upper dark line (HT); lower grey line
              (PCT). Arrows point to the border of the cuticle. Bar: 50 μm.

3.2 Comparison of different tissues

A part of the internal reproductive system (ovary, oocytes during vitellogenesis, eggs) was compared (Fig. 3). The grey values ranged from 0 to 238 for PCT (max.: 101, mean: 102.2, SD: 21.3) and from 0 to 243 for HT (max.: 220, mean: 152.2, SD: 52.8). The distribution of grey values was peak-shaped for PCT but had two maxima (one for the background, one for the sample) and a quite complex shape for HT.

A part of the ventriculus with ventricular cells, cells of the epidermis and a part of the cuticle, was compared (Fig. 4). Again, HT had two peaks and a more complex distribution of grey values than PCT. The range for PCT was between 48 and 214 (max.: 101, mean: 102, SD: 18.8). Grey values of HT ranged from 32 to 227 (max.: 172, mean: 150.9, SD: 40.7). While HT allowed a clear differentiation between ventricular and epidermal cells, there was no detectable clear border in PCT.

The grey value distribution of a virtual slice of the synganglion (representing the nervous system) showed the same principal results (Fig. 5). With a range of 42 to 222 (max.: 104, mean: 102.4, SD: 17.8), the PCT slice allowed no clear differentiation of different parts of the synganglion. The HT image had grey values between 27 and 214 (max.: 95, mean: 121.8, SD: 34.2) with three local maxima (one for the background, two for the sample) and it was easy to differentiate between different functional parts.
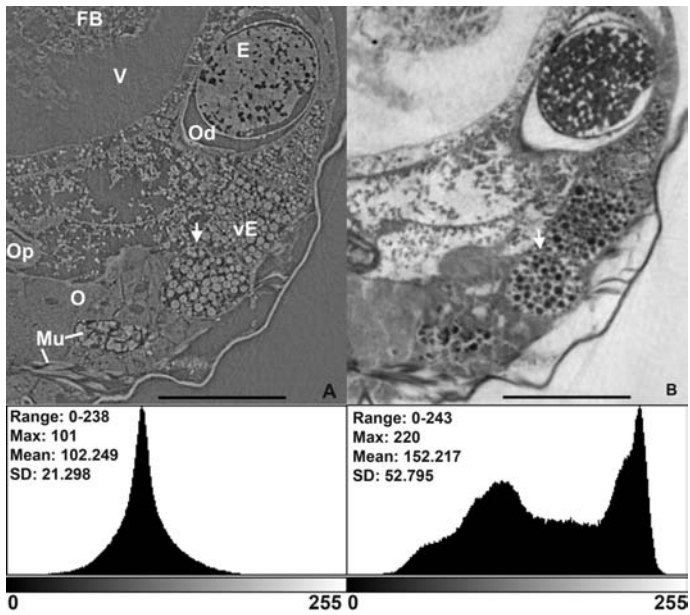
Fig. 3   Comparison of grey value distribution in virtual slices of PCT and HT in the region of the reproductive system with corresponding histograms. A: PCT; B: HT; E: egg; FB: food bolus; Mu: muscles; O: ovary; Od: ovicuct with free lumen; Op: ovipositor; vE: eggs during vitellogenesis. Arrows point to the border between two vitellogenetic oocytes. Bar: 100 µm.
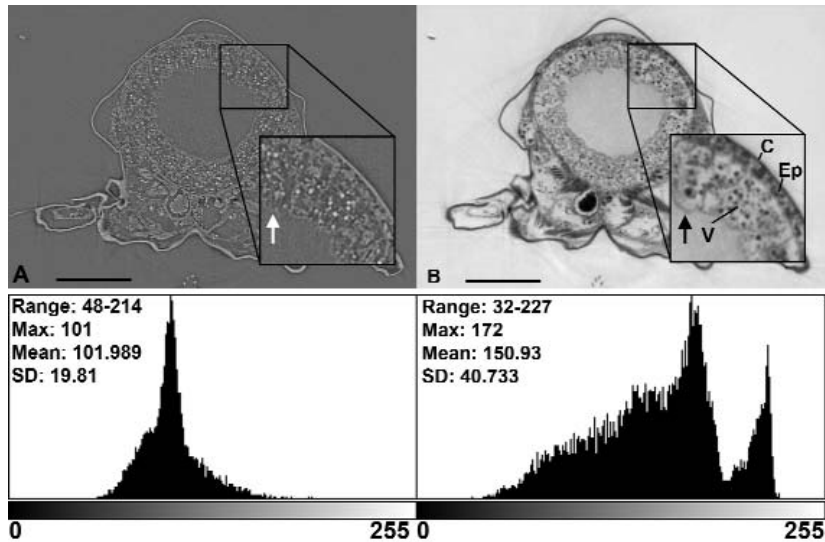
Fig. 4   Comparison of grey value distribution in virtual slices of PCT and HT in the region of the ventricular wall with corresponding histograms. A: PCT; B: HT; C: cuticle; Ep: epidermis; v: ventricular wall. Arrows point to the microvilli. Bar: 100 µm.
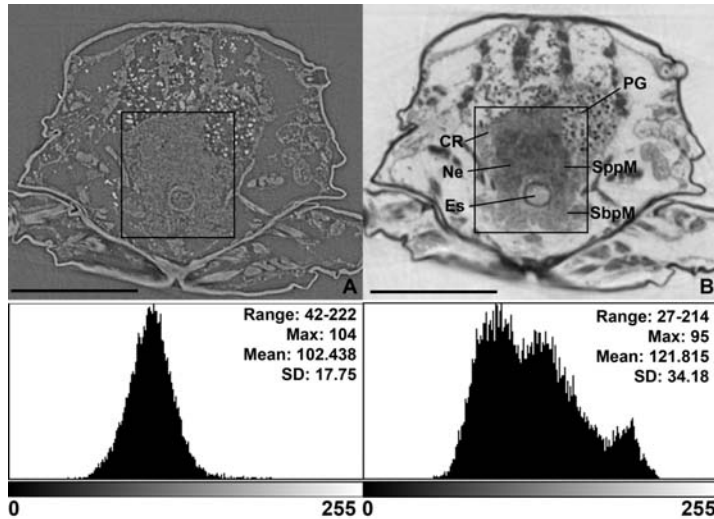
Fig. 5   Comparison of grey value distribution in virtual slices of PCT and HT in the region of the
          synganglion with corresponding histograms (histograms correspond to the region in the
          black box). A: PCT; B: HT; CR: cortical region; Es: oesophagus; Ne: neuropile; PG:
          preventicular gland; SbpM: suboesophageal mass; SppM: supraoesophageal mass. Bar: 100
          μm.

4. Discussion

4.1. General comparison of phase contrast tomography (PCT) and holotomography (HT)

The distribution of grey values in the background provides, when compared to the grey values of the sample, important information on the signal-to noise ratio. Since the sample rotates during the scanning procedure, the reconstructed virtual slices have a circular interior appearance (coming from the sample and the surrounding air) with an artificial sharp uniform grey value in the corners to obtain square-shaped slices. This grey value is responsible for the sharp maxima in the virtual slices (* in Fig. 1). The maximum grey values always differed only by 1 after removing the corner-background. Hence, there is no large difference in grey value distribution with or without the artificial corner. However, only details within the circular sample area were used for subsequent analyses.

The maximum grey value of the PCT background (Fig. 1A) was 102, which was close to the mean value of 101. The PCT sample (Fig. 1B) had a mean of 101.8 with a standard deviation of 11.4. This means that the grey values of the sample are distributed closely to the maximum and mean values of the background. Thereby much information of the sample is blurred and superimposed by the background. The HT background (Fig. 1C) has a mean grey value of 215.4 which is 14 steps away from the mean value of the sample (201.6). Also, the standard deviation of the grey value distribution in the HT sample is almost four times higher than in the PCT slice. Hence, the grey value distribution in the HT sample is less superimposed by the background and contains more differential information. This becomes

obvious when all grey values from the background are subtracted from the slice containing the sample (Fig. 6). Except for the cuticle and some basic information on interior tissues, the PCT image lost most of the information during background subtraction (Fig. 6A). In contrast, the HT image easily allows the differentiation of internal tissues even after the subtraction of all background grey values (Fig 6B).
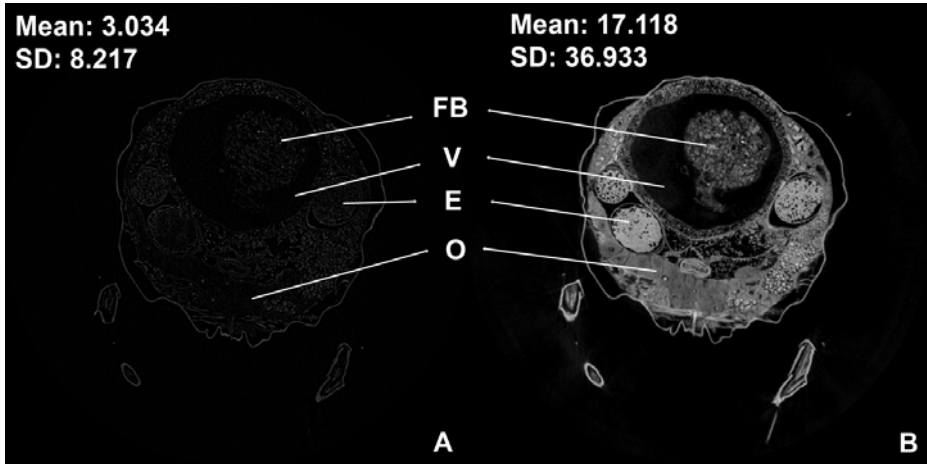
Fig. 6   Comparison of grey value distribution in virtual slices of PCT and HT after subtraction of all grey values from the background. A: PCT; B: HT; E: egg; FB: food bolus; O: ovary; V: ventriculus.

The effect of edge-enhancement is the core of PCT (Cloetens et al. 1996). Here, borders of different materials are enhanced by a dark layer, which is visible in the grey value distribution along the border of the cuticle (Fig. 2). When different phase contrast scans are combined into a single phase map, which is subsequently used for HT, this edge enhancement is removed (Cloetens et al. 2007). Hence, the reconstruction of the virtual slices with HT is less prone to artificial edge enhancement.

4.2. Comparison of different tissues

The internal reproductive system of *A. longisetosus* consists of an unpaired ovary with two branches, two oviducts and an unpaired cuticular ovipositor (Heethoff et al. 2007). The oocytes inside the ovary have a homogeneous interior, and grow on their way from the central zone to the oviducts. During vitellogenesis, the oocytes become filled with nutritive vesicles and lose their homogeneous appearance. After vitellogenesis, the eggs are encapsulated in a vitellar membrane and a chorion and the embryo starts to develop. No free lumen can be detected among the oocytes until the completion of vitellogenesis; then the eggs are surrounded by a free lumen in the oviducts (Fig. 3). The grey value distribution differs strongly between PCT and HT in these slices. In the PCT slice, the mean value of 102.2 (SD: 21.3) is again close to the maximum of 101 which is a characteristic grey value for the PCT background. In contrast, the HT mean value of 152.2 (SD: 52.8) is more than 60 steps

away from the mean grey value of the background (215.4), and the standard deviation of grey values is 2.5 times higher than that of PCT. Hence, it is possible to differentiate between a wide range of specific tissue densities with HT, which are denoted by the same grey values in PCT. However, the effect of edge enhancement also has some advantages: It is easier to detect some borders with PCT, although the information on the internal structure of the tissue is better with HT. For example, the border between vitellogenetic oocytes can be detected in the PCT slice, but not in the HT slice (see arrows in Fig. 3).

The digestive tract of oribatid mites comprises a cuticular foregut (mouth, pharynx, oesophagus), a midgut (ventriculus, preventricular glands, a pair of caecae, a colon, an intercolon and a postcolon), and a cuticular hindgut terminating with the anus. The wall of ventriculus consists of a single cell type, which might have variable appearance due to different physiological states of the cells and contain granules of composed layers of dense and less dense material (spherites) and lysosomes (Alberti et al. 2003). The cells are provided with microvilli on the side of the ventricular lumen. The PCT slice again had a grey value distribution close to that of the background (102) and a standard deviation of 19.8. The HT slice had two peaks in this region. One was located at 220 and referred to the background; the other one had a maximum grey value of 172 which referred almost exclusively to the sample. The standard deviation of the grey value distribution was twice as high as with PCT. In the HT slice, the microvilli are detectable as a soft layer on the ventricular cells (black arrow, Fig. 4B), which is not the case in the PCT slice (white arrow, Fig. 4A); spherites in the ventricular cells can be detected by both methods. Ventricular and epidermal cells can simply be differentiated in the HT image but not in the PCT slice. This illustrates the benefit of holotomography: Differential imaging of neighbouring soft tissues with only slight differences in X-ray density and without a sharp border in between.

The nervous system of arthropods is characterised by a ventral chain of ganglia. These ganglia exhibit various degrees of fusion in different taxonomic groups. The Acari are characterised by a fusion of all ganglia into a single mass: the synganglion (Coons & Axtell 1971, Alberti & Coons 1999). The oesophagus passes through the synganglion and divides it into a dorsal supraoesophageal mass (innervation of the pharynx and the chelicerae) and a ventral suboesophageal mass (innervation of pedipalps, legs and posterior organs). Like in other arthropods, the synganglion consists of an outer cortical region and an inner neuropile. The cortical region consists of layers of glial cells and neural cell bodies; the neuropile contains nerve fibres and glial cells. The distribution of grey values was compared in the region of the synganglion only (black box in Fig. 5). Comparable to all other regions, the mean grey value distribution of PCT was close to that of the background with a standard deviation of 17.8. It was not possible to differentiate between different functional regions (cortical region and neuropile) of the synganglion. The HT reconstruction has a mean grey value of 121.8 (almost 100 steps away from the background) and a standard deviation of 34.2 (Fig. 5A). The cortical region and the neuropile can easily be differentiated due to their different grey value distribution and are characterised by two maxima in the histogram (Fig. 5B).

To conclude, PCT is a powerful method to generally detect tissues with low attenuation coefficients (no absorption) or borders between different tissues, but is not suitable to detect small difference of X-ray densities within tissues. The reason for this is that the signal-to-noise ratio is quite low and that much of the information is blurred by the background. In contrast to this, HT offers the opportunity to differentiate between tissues with only slight differences in attenuation coefficients. The signal-to-noise ratio is much higher than with PCT, demonstrated by higher standard deviations of grey value distributions and by a lower overlap of background and sample grey values. The appearance of HT slices is comparable to histological sections with single staining, observed by a light microscope. Hence, HT is a powerful method for the analyses of microarthropods with the advantages that it is fast, non-destructive, and has a high spatial and differential resolution.

5. Acknowledgements

6. References

Alberti, G. & L. B. Coons (1999): Acari – Mites. – In: Harrison, F. W. (ed.): Microscopic Anatomy of Invertebrates. Vol. **8** C. – John Wiley & Sons, Inc., New York: 515 – 1265

Alberti, G., A. Seniczak & S. Seniczak (2003): The digestive system and fat body of an early-derivative oribatid mite, *Archegozetes longisetosus* Aoki (Acari: Oribatida, Thrypochthoniidae). – Acarologia **43**: 149 – 219

Betz, O., U. Wegst, D. Weide, M. Heethoff, L. Helfen, W.-K. Lee & P. Cloetens (2007): Imaging applications of synchrotron X-ray phase-contrast microtomography in biological morphology and biomaterial science. I. General aspects of the technique and its advantages in the analysis of millimetre-sized arthropod structure. – Journal of Microscopy **22**: 51 – 71

Cloetens, P., R. Mache, M. Schlenker & S. Lerbs-Mache (2007): Quantitative phase tomography of *Arabidopsis* seeds reveals intercellular void network. – Proceedings of the National Academy of Sciences of the United States of America **103**: 14626 – 14630

Cloetens, P., R. Barrett, J. Baruchel, J. P. Guigay & M. Schlenker (1996): Phase objects in synchrotron radiation hard X-ray imaging. – Journal of Physics D: Applied Physics **29**: 133 – 146

Coons, L. B. & R. C. Axtell (1971): Cellular organization in the synganglion of the mite *Macrocheles mescadomesticae* (Acarina: Macrochelidae). – Zeitschrift für Zellforschung **119**: 309 – 320

Heethoff, M., M. Laumann & P. Bergmann (2007): Adding to the reproductive biology of the parthenogenetic oribatid mite *Archegozetes longisetosus* (Acari, Oribatide, Trhypochthoniidae). – Turkish Journal of Zoology **31**: 151 – 159

Radon, J. (1917): Über die Bestimmung von Funktionen durch ihre Integralwerte längs gewisser Mannigfaltigkeiten. – Berichte der Sächsischen Akademie der Wissenschaften **29**: 262 – 277

Weide, D. & O. Betz (2007): Anwendung der Synchrotron Mikro-Röntgentomographie (SR-μCT) in der Insektenmorphologie. – Mitteilungen der Deutschen Gesellschaft für allgemeine und angewandte Entomologie **16**: 467 – 472